Theoretical Study on the Reactivities of Stannylene and Plumbylene and the Origin of their Activation Barriers

Ming-Der Su*[a]

Abstract: The potential energy surfaces corresponding to the reactions of heavy carbenes with various molecules were investigated by employing computations at the B3LYP and CCSD(T) levels of theory. To understand the origin of barrier heights and reactivities, the model system $(CH_3)_2X+Y$ (X = C, Si, Ge, Sn, and Pb; Y = CH_4, SiH_4, GeH_4, CH_3OH, C_2H_6, C_2H_4, and C_2H_2) was chosen for the present study. All reactions involve initial formation of a precursor complex, followed by a high-energy transition state, and then a final product. My theoretical investigations suggest that the heavier the X center, the larger the activation barrier, and the less exothermic (or the more endothermic) the chemical reaction. In particular, the computational results show that $(CH_3)_2Sn$ does not insert readily into C–H, Si–H, C–H, Ge–H, or C–C bonds. It is also unreactive towards C=C bonds, but is reactive towards C≡C and O–H bonds. My theoretical findings are in good agreement with experimental observations. Furthermore, a configuration mixing model based on the work of Pross and Shaik is used to rationalize the computational results. It is demonstrated that the singlet–triplet splitting of a heavy carbene $(CH_3)_2X$ plays a decisive role in determining its chemical reactivity. The results obtained allow a number of predictions to be made.

Keywords: carbene homologues · cycloaddition · density functional calculations · Group 14 elements · insertion

Introduction

Divalent molecules of the Group 14 elements, such as carbenes (R_2C),[1] silylenes (R_2Si),[2] and germylenes (R_2Ge),[3] have long been the subject of intense experimental and theoretical investigation. The structures and reactivity of the corresponding divalent tin species, stannylenes (R_2Sn), have gained increasing attention in recent years.[4] Thus, X-ray crystallographic studies have resulted in the structural characterization of numerous substituted stannylenes bearing various ligands R.[5,6] The study of the chemical reactivity of stannylenes has also led to the synthesis of many intriguing molecules.[7] Nevertheless, the detailed reaction mechanisms for such reactions have not been firmly established by either experimental or theoretical studies, and many key questions remain open.

The principal motivation for this research was a remarkable recent experimental discovery by Walsh et al.[8] who, using a laser flash photolysis/laser probe technique, showed that Me_2Sn does not insert readily into C–H, Si–H, Ge–H, C–C, Si–C, or Ge–C bonds. It is also unreactive towards alkenes, although not towards dienes or alkynes. These experimental observations are quite different from those made for carbenes,[9] silylenes,[10] and germylenes.[11] In fact, it is well known that silylenes and germylenes, like carbenes, can undergo insertions into a variety of σ bonds and cycloadditions with various kinds of π bonds. Accordingly, there is a desire to understand the fundamental chemistry of stannylenes and how their reactions compare to those of its Group 14 analogues. Indeed, comparison of the behavior of stannylenes with their carbon, silicon, and germanium analogues reveal how the mechanistic principles developed for organic chemistry can be extended to deal with bond-making and bond-cleavage processes for elements lying further down the Periodic Table (vide infra).

Hence, attention has inevitably also been directed towards the reactivity of divalent plumbylenes (R_2Pb).[12] Despite the considerable interest in carbene, silylene, and germylene chemistry over the past thirty years, the chemistry of stannylenes and plumbylenes has not been similarly investigated. This is presumably a result of the instability inherent to electron-deficient divalent species, and the fact that both have not been easily accessible by the synthetic routes conventionally used in the preparation of carbenes, silylenes, and germylenes. As far as I am aware, theoretical analyses of crucial stannylene and plumbylene reactions are still greatly lacking, with the exception of some work by Dewar,

[a] Prof. M.-D. Su
School of Medicinal and Applied Chemistry
Kaohsiung Medical University
Kaohsiung 80708, Taiwan (Republic of China)
Fax: (+886) 07-3125339
E-mail: midesu@cc.kmu.edu.tw

 DOI: 10.1002/chem.200400413

et al.[13a] and Sakai.[13b] In these theoretical studies only the latter proposed a simple singlet excitation model for the transition states (TSs) of stannylenes with ethylene to rationalize the heights of their energy barriers.

If the basic factors governing the chemical reactivity of various carbene analogues with organic molecules could be understood, this would help to design systems which facilitate these synthetically useful, but presently unattainable, reactions. My aim is therefore to search for a general theory of reactivity for carbene and its heavier analogues and to delineate the significant role played by their singlet–triplet energy separations (vide infra). To mimic the experimental observations of Walsh et al.,[8] I calculated the potential energy surfaces of five insertion reactions [Eqs. (1)–(5)] and two addition reactions [Eqs. (6)and (7)].

$$CH_4 + Me_2X \rightarrow Me_2(H)X{-}CH_3 \quad (1)$$

$$SiH_4 + Me_2X \rightarrow Me_2(H)X{-}SiH_3 \quad (2)$$

$$GeH_4 + Me_2X \rightarrow Me_2(H)X{-}GeH_3 \quad (3)$$

$$CH_3OH + Me_2X \rightarrow Me_2(H)X{-}OCH_3 \quad (4)$$

$$CH_3CH_3 + Me_2X \rightarrow Me_2(CH_3)X{-}CH_3 \quad (5)$$

$$H_2C{=}CH_2 + Me_2X \rightarrow \begin{array}{c} Me_2X \\ / \quad \backslash \\ H_2C \quad CH_2 \end{array} \quad (6)$$

$$HC{\equiv}CH + Me_2X \rightarrow \begin{array}{c} Me_2X \\ / \quad \backslash \\ HC{=}CH \end{array} \quad (7)$$

(X = C, Si, Ge, Sn, Pb)

No systematic theoretical study has yet, to my knowledge, been published on the potential energy surfaces and reaction mechanisms of insertion and cycloaddition reactions of stannylenes and plumbylenes. Thus, in this work I attempted to study such reactions of heavier carbenes using both DFT and the ab initio CCSD(T) methods. On the basis of these computational results, I show that the singlet–triplet splitting of carbene analogues can be used as a diagnostic tool for the prediction of their reactivity.

The Origin of the Barrier and Reaction Enthalpy for Me_2X Reactions

To highlight the questions which formed the basis of this study, it is worthwhile to review briefly the origin of barrier height and reaction enthalpy. Indeed, the question of the origin of barriers to chemical reactions, and of how their heights may be predicted, lies at the heart of the understanding of chemical processes. The following attempts to provide a qualitative explanation for the source of the activation energy. This explanation is based on the general conclusions which Pross and Shaik arrived at with the aid of the configuration mixing (CM) model.[14,15] Within this model, all possible configurations involving the frontier orbitals of the individual reacting molecules are formed, and the wavefunctions along the reaction coordinate are analyzed in terms of these configurations. As a result, in the σ-bond insertion (or cycloaddition) reaction, the system can exist in a number of predetermined states, each of which can be approximated by the appropriate electronic configuration.[14,15] However, there are only two predominant configurations that contribute significantly to the total wavefunction Ψ and, in turn, affect the shape of the potential energy surface. As one can see in Figure 1, we can represent the qualitative be-

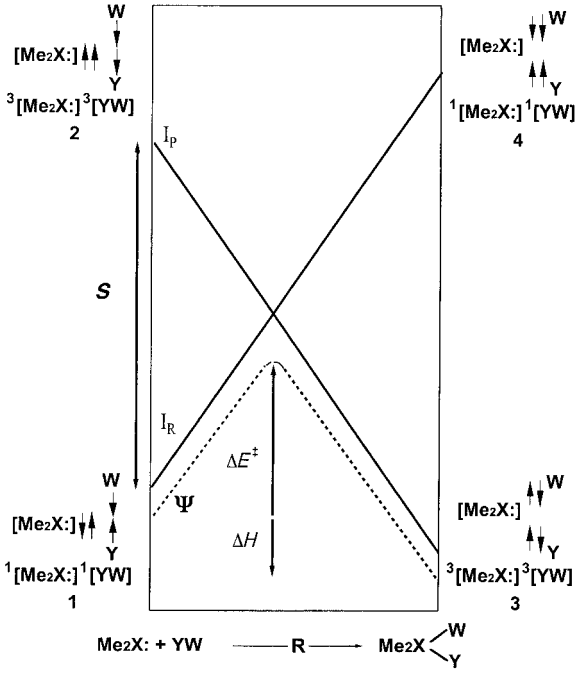

Figure 1. Energy diagram for a chemical reaction showing the formation of a state curve Ψ by mixing two configurations: the reactant configuration I_R and the product configuration I_P. In the reactants, they are separated by an energy gap *S*. Configuration mixing near the crossing point causes avoidance of crossing (dotted line).

havior of the two configurations for the insertion of Me_2X species into a Y–W bond. One is the reactant ground-state configuration, which ends up as an excited configuration in the product region. The other is the excited configuration of the reactants, which correlates with the ground state of the products. These two components are denoted as the reactant configuration I_R and the product configuration I_P, respectively.

The key valence bond (VB) configurations for Me_2X insertion are illustrated in **1** and **2**. The VB configuration **1**, labeled $^1[Me_2X]^1[YW]$, is termed the reactant configuration I_R because this configuration is a good description of the reactants; the two electrons on the Me_2X moiety are spin-paired to form a lone pair, while the two electrons on the YW moiety are spin-paired to form a Y–W σ bond. On the other hand, configuration **2** is the VB product configuration I_P. Note that the spin arrangement is now different. The electron pairs are coupled to allow both X–Y and X–W bond formation and simultaneous Y–W bond breaking. To obtain this configuration from the reactant configuration **1**, each of the two original electron pairs must be uncoupled, that is, these two electron pairs require excitation from the singlet to the triplet state. Hence, this configuration is labeled

$^3[Me_2X]^3[YW]$. The molecular orbital (MO) representations of VB configurations **1** and **2** are **3** and **4**, respectively.

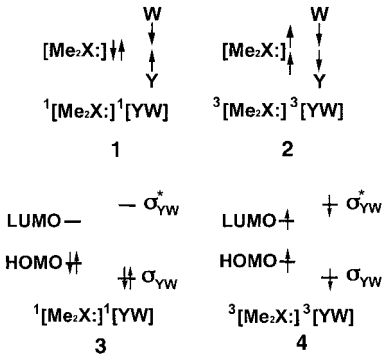

On the basis of these considerations, I propose that the transition state for the insertion reaction of Me_2X into a Y–W bond is composed of the respective triplet states of the reactants, which couple to give an overall singlet state. At first glance, it might appear that promotion to such a valence state requires too much energy. However, it will be shown below that such a promotion is indeed feasible. Before further discussion, let us emphasize the importance of the status of the triplet state for the Me_2X and Y–W reactants. Since two new covalent bonds are formed in the product $Me_2X(Y)(W)$, that is, the X–Y and X–W bonds, the bond-prepared Me_2X state thus must have at least two open shells, and the lowest state of this type is the triplet state. Therefore, from the valence-bond point of view, the bonding in the product can be recognized as that between the triplet Me_2X state and two doublet radicals (overall singlet), that is, the Y radical and the W radical. This is much the same as the bonding in the water molecule, which can be considered as that between a triplet oxygen atom and two doublet hydrogen atoms.[17]

At this point, it is interesting to note that the singlet–triplet excitation energy mentioned above plays a decisive role in the CM model (schematically illustrated in Figure 1), proposed by Pross and Shaik for understanding barrier formation in chemical reactions.[14,15] The singlet–triplet excitation energy corresponds to the energy gap E in the CM model between the reactant configuration I_R and product configuration I_P. In the reactants, I_R is the ground state of the system, whereas I_P is an excited state at an energy E above I_R. As the reaction proceeds, the energy of I_R rises and that of I_P drops. The transition state is reached at a point along the reaction coordinate at which the energy curves of I_R and I_P cross. The reaction system reaches a maximum energy somewhat below this crossing point, due to avoided crossing of I_R and I_P; this is indicated by the dotted curve in Figure 1. Finally, in the products the roles of I_R and I_P have been inverted. That is, I_R becomes the excited-state configuration, and I_P a ground state. As a consequence, it is the avoided crossing of these two configurations that leads to the simplest description of the ground state energy profiles for chemical reactions of carbenes and their analogues.[11,14–16]

Based on Figure 1 for barrier formation in chemical reactions, we are now in a position to provide an insight into the parameters that are likely to affect reactivity in this system. The energy of point **2** (left-hand side of Figure 1), the anchor point for $^3[Me_2X]^3[YW]$ in the reactant geometry, will be governed by the singlet–triplet energy gap for both Me_2X and Y–W, that is, ΔE_{st} ($=E_{triplet}-E_{singlet}$ for Me_2X) + $\Delta E_{\sigma\sigma^*}$ ($=E_{triplet}-E_{singlet}$ for Y–W). Note that the barrier of the chemical reaction is caused by the promotion energy S, which is nonzero, as shown in Figure 1. The decrease in S ($S=\Delta E_{st}+\Delta E_{\sigma\sigma^*}$) also stabilizes the product and makes the reaction enthalpy ΔH more exothermic.[18] In other words, the smaller the promotion energy S, the lower the activation barrier, and the larger the exothermicity.[14,15] For this reason, if a reactant Me_2X has a singlet ground state with a small triplet excitation energy, it offers a greater opportunity for involvement of triplet Me_2X in the singlet reaction, and such reactions will occur readily.

One can thus conclude that both the order of the singlet and triplet states as well as the magnitude of the singlet–triplet energy separation are responsible for the existence and height of the energy barrier. Bearing the above analysis (Figure 1) in mind, the origin of the observed trends which are described in the following section will be explained.[19]

Results and Discussion

Geometries and energetics of Me_2X: Before discussing the geometrical optimizations and potential energy surfaces for the chemical reactions studied in the present work, we shall first discuss the geometries and energies of the dimethyl-substituted Group 14 divalent reactants Me_2X. The electronic structures and geometries of such divalent species have been extensively studied by many groups. In this work, selected geometrical values for singlet and triplet Me_2X as well as the triplet energies relative to the singlet reactants based on the B3LYP and CCSD(T) levels are given in Table 1.

Table 1. Geometrical parameters and relative energies for singlet and triplet Me_2X species (X = C, Si, Ge, Sn, Pb).[a,b]

System	X–C (singlet) [Å]	∢CXC (singlet) [°]	X–C (triplet) [Å]	∢CXC (triplet) [°]	ΔE[c] [kcal mol^{-1}]
$(CH_3)_2C$	1.505	112.7	1.492	133.6	−4.951 [−0.4651]
$(CH_3)_2Si$	1.931	97.82	1.918	119.1	+21.59 [+22.00]
$(CH_3)_2Ge$	2.209	95.62	2.012	117.6	+27.64 [+26.91]
$(CH_3)_2Sn$	2.197	93.58	2.192	116.7	+29.36 [+27.93]
$(CH_3)_2Pb$	2.267	93.02	2.239	116.9	+36.99 [+36.49]

[a] At the B3LYP/LANL2DZ [CCSD(T)/LANL2DZdp//B3LYP/LANL2DZ] levels of theory. [b] Energy differences have been zero-point-corrected. See text. [c] Energy relative to the corresponding singlet state. A positive value means the singlet is the ground state.

An interesting trend that can be observed in Table 1 is the decrease in the X–CH_3 bond lengths and the increase in the ∢CXC bond angles on going from the singlet to the triplet state. The reason for this can be understood simply by con-

sidering their electronic structures.[9,14,15] The other intriguing feature is the singlet–triplet splittings ($\Delta E_{st} = E_{triplet} - E_{singlet}$). The DFT and CCSD(T) calculations (in parentheses) indicate that the singlet–triplet splittings for dimethyl-substituted carbene, silylene, germylene, stannylene, and plumbylene are −5.0 (−0.47), 22 (22), 28 (27), 29 (28), and 37 (36) kcal mol^{-1}, respectively. That is, ΔE_{st} increases in the order $Me_2C < Me_2Si < Me_2Ge < Me_2Sn < Me_2Pb$, and thus follows the same trend as the electronegativity of the central atom X. Apparently, the heavier Group 14 elements are pivotal atoms in this regard. These results are consistent with those reported in the previous studies cited above, and will not be discussed further. Finally, as shown in Table 1, all the Me_2X species are predicted to have singlet (or nearly singlet) ground states according to both DFT and CCSD(T) computational results. This strongly implies that all the chemical reactions [Eqs. (1)–(7)] studied in this work should proceed on the singlet surface, and thus the focus will be on the singlet surface from now on.

Basically, the chemical reactions studied in this work follow the general reaction path as shown in Scheme 1. The Me_2X species attacks an organic molecule to form a precursor complex, which then rearranges to yield the eventual product via a TS. Thus, four stationary points on the potential energy surfaces are considered: Me_2X (X = C, Si, Ge, Sn, and Pb) plus an organic molecule, the precursor complex, the TS, and the final product. Experimental geometries for the above stationary points are not yet available, and it is hard to determine the accuracy of stationary-point geometries generated by computational methods. Nevertheless, the prediction of geometrical parameters seems to be consistent with changing level of theory. Moreover, as can be seen in the tables shown below, the trends for both B3LYP and CCSD(T) results are qualitatively the same. This means that the use of the latter is sufficient to provide qualitatively correct results. This work is primarily concerned with discovering the key factors that affect the reactivity of heavy carbene species, and thus, unless otherwise noted, only the CCSD(T) energetic results are used in the following discussion for the sake of convenience.

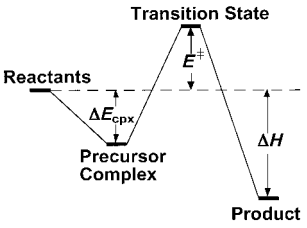

Scheme 1.

Methane insertion reactions: The geometries and energetics of the stationary points shown in **5** for methane insertion reactions [Eq. (1)] were calculated with the B3LYP and CCSD(T) methods. The fully optimized geometries for these stationary points, calculated at the B3LYP/LANL2DZ level, are given in Figure 2. The relative energies of these stationary points based on B3LYP and CCSD(T) methods are also summarized in Table 2. The major conclusions that can be drawn from Table 2 and Figure 2 follow.

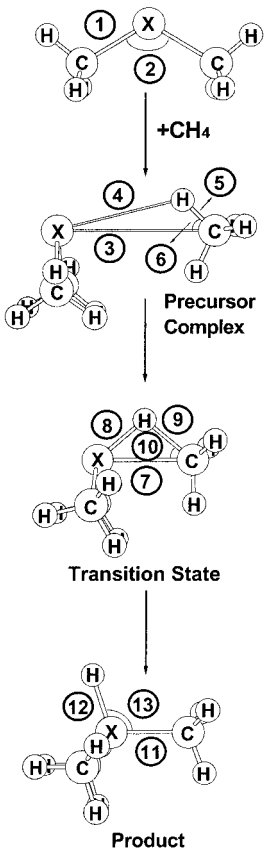

	C	Si	Ge	Sn	Pb
1	1.506	1.931	2.209	2.197	2.267
2	112.7	97.82	95.62	93.58	93.02
3	3.680	3.905	3.635	3.866	3.861
4	2.691	3.137	2.960	3.145	3.163
5	1.097	1.097	1.097	1.098	1.098
6	21.58	39.46	44.84	42.51	43.91
7	2.363	2.349	2.402	2.527	2.571
8	1.345	1.533	1.578	1.733	1.752
9	1.254	1.545	1.654	1.777	1.935
10	25.58	40.06	40.79	42.94	43.28
11	1.546	1.900	1.976	2.146	2.202
12	1.103	1.494	1.556	1.727	1.758
13	108.0	108.4	108.7	108.9	109.0

Figure 2. B3LYP/LANL2DZ-optimized geometries [Å, °] of the reactants (singlet), precursor complexes, transition states, and insertion products of $(CH_3)_2X$ (X = C, Si, Ge, Sn, and Pb) and CH_4.

The B3LYP frequency calculations for these transition states show that the single imaginary frequency values are

Table 2. Relative energies for singlet and triplet carbenes and for the process reactants ($(CH_3)_2X + CH_4$)→precursor complex→transition state→insertion product.[a,b]

System	ΔE_{st}[c] [kcal mol^{-1}]	ΔE_{cpx}[d] [kcal mol^{-1}]	ΔE^{+}[e] [kcal mol^{-1}]	ΔH[f] [kcal mol^{-1}]
$(CH_3)_2C$:	−0.4651	−0.4586	+6.659	−83.46
	(−4.951)	(−0.1738)	(+6.603)	(−81.78)
$(CH_3)_2Si$:	+22.00	−0.7964	+22.69	−51.59
	(+21.59)	(−0.1242)	(+27.72)	(−44.33)
$(CH_3)_2Ge$:	+26.91	−1.039	+33.31	−30.82
	(+27.64)	(−0.1079)	(+36.25)	(−28.23)
$(CH_3)_2Sn$:	+27.93	−1.138	+44.16	−3.700
	(+29.36)	(−0.1418)	(+46.60)	(−2.624)
$(CH_3)_2Pb$:	+36.49	−1.211	+57.11	+10.05
	(+36.96)	(−0.6275)	(+59.98)	(+11.43)

[a] At the CCSD(T)/LANL2DZdp//B3LYP/LANL2DZ (B3LYP/LANL2DZ) levels of theory. For B3LYP-optimized structures of the stationary points, see Figure 2. [b] Energies differences have been zero-point-corrected. See text. [c] Energy relative to the corresponding singlet state. A positive value means the singlet is the ground state. [d] Stabilization energy of the precursor complex, relative to the corresponding reactants. [e] Activation energy of the transition state, relative to the corresponding reactants. [f] Reaction enthalpy of the product, relative to the corresponding reactants.

665*i* (Me_2C-TS), 1214*i* (Me_2Si-TS), 1174*i* (Me_2Ge-TS), 1114*i* (Me_2Sn-TS), and 985*i* cm^{-1} (Me_2Pb-TS). Examination of the single imaginary frequency for each TS provides an excellent confirmation of the concept of an insertion process. These insertion reactions appear to be concerted, because I was able to locate only one TS for each reaction and confirmed that it is a true TS on the basis of frequency analysis. The transition structures for the insertion of Me_2X into CH_4 for various central atoms X are very similar. The computational results show that the primary similarity among these transition structures is the three-center pattern involving central X, carbon, and hydrogen atoms. Such characteristic three-center transition states are in accordance with mechanisms postulated by Su and Chu.[11] In addition, our model calculations show that all the insertion products adopt a staggered, ethane-like structure.

A comparison of the aforementioned five species reveals several interesting trends. According to the CM model discussed earlier, the stabilization of an insertion transition state depends on the singlet–triplet splitting ΔE_{st} ($=E_{triplet}-E_{singlet}$) of the carbene reactant; that is, a smaller ΔE_{st} results in a more stable transition state, a lower activation energy, and a faster insertion reaction. Our model calculations confirm this prediction, and suggest an increasing ΔE_{st} in the series $Me_2C < Me_2Si < Me_2Ge < Me_2Sn < Me_2Pb$. From Table 2, it can be seen that this result is in good agreement with the trend in activation energies (kcal mol^{-1}): Me_2C-TS (+6.7) < Me_2Si-TS (+23) < Me_2Ge-TS (+33) < Me_2Sn-TS (+44) < Me_2Pb-TS (+57). Also, the order of reaction enthalpy (kcal mol^{-1}) follows the same trend as the ΔE_{st} of Me_2X Me_2C-Pro (−83) < Me_2Si-Pro (−52) < Me_2Ge-Pro (−31) < Me_2Sn-Pro (−3.7) < Me_2Pb-Pro (+10). These data strongly imply that the value of ΔE_{st} is a remarkably diagnostic tool of the reactivity of a Me_2X species.[14,15] Note that the energy of Me_2Pb-Pro is higher than that of its corresponding reactants. This indicates that insertion of plumbylene into methane is endothermic and would be energetically unfavorable. Stannylene insertion into methane is predicted to be nearly thermoneutral, with an exothermicity of less than 4 kcal mol^{-1}. This computational result is consistent with the experimental observation that Me_2Sn is unreactive towards C–H bonds.[8] Likewise, my theoretical findings also suggest that Me_2Ge does not insert readily into the C–H bond, which has been confirmed by experimental works.[20]

Silane insertion reactions: The geometrical results from the theoretical study on silane insertion reactions [Eq. (2)] are collected in Figure 3. The relative energies of the stationary points shown in **5** are summarized in Table 3. The major conclusions that can be drawn from Table 3 and Figure 3 are given below.

Again, only one TS could be located for each silane insertion reaction, and it was confirmed that it is a true TS on the basis of frequency analysis. Examination of the single imaginary frequency for each transition state [121*i* (Me_2C-TS), 800*i* (Me_2Si-TS), 814*i* (Me_2Ge-TS), 797*i* (Me_2Sn-TS), and 690*i* cm^{-1} (Me_2Pb-TS)] provides an excellent confirmation of the concept of the SiH_4 insertion process; that is, the reactants approach each other with their molecular planes perpendicular, and two new bonds are formed at the same time. Let us now consider the effect of singlet–triplet splitting. Clearly, the smaller ΔE_{st} (Me_2X), the lower the activation energy and the lower the heat of the silane insertion reaction. For instance, as demonstrated in Table 3, since ΔE_{st}

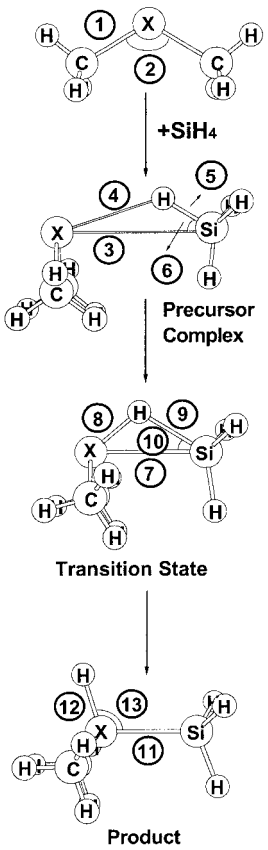

	C	Si	Ge	Sn	Pb
1	1.506	1.931	2.209	2.197	2.267
2	112.7	97.82	95.62	93.58	93.02
3	3.680	3.905	3.635	4.610	3.861
4	4.483	3.264	3.360	4.162	3.721
5	1.481	1.481	1.486	1.481	1.492
6	75.06	62.07	54.05	56.42	60.07
7	3.332	2.839	2.844	2.973	2.964
8	1.878	1.557	1.602	1.761	1.780
9	1.520	1.912	2.030	2.158	2.364
10	12.62	31.15	33.37	35.89	36.90
11	1.914	2.355	2.419	2.600	2.633
12	1.102	1.492	1.554	1.729	1.755
13	107.1	107.7	108.1	108.3	109.0

Figure 3. B3LYP/LANL2DZ-optimized geometries [Å, °] of the reactants (singlet), precursor complexes, transition states, and insertion products of $(CH_3)_2X$ (X = C, Si, Ge, Sn, Pb) and SiH_4.

Table 3. Relative energies for singlet and triplet carbenes ($(CH_3)_2X$) and for the process: reactants ($(CH_3)_2X+SiH_4$)→precursor complex→transition state→insertion product.[a,b]

System	ΔE_{st}[c] [kcal mol^{-1}]	ΔE_{cpx}[d] [kcal mol^{-1}]	$\Delta E^{\neq}$[e] [kcal mol^{-1}]	ΔH[f] [kcal mol^{-1}]
$(CH_3)_2C$:	−0.4651	−0.5829	+1.545	−86.12
	(−4.951)	(−0.7906)	(+1.855)	(−87.67)
$(CH_3)_2Si$:	+22.00	−1.085	+6.300	−51.69
	(+21.59)	(−0.3220)	(+10.63)	(−46.56)
$(CH_3)_2Ge$:	+26.91	−1.399	+14.72	−35.15
	(+27.64)	(−0.5993)	(+17.15)	(−33.91)
$(CH_3)_2Sn$:	+27.93	−1.388	+24.74	−10.84
	(+29.36)	(−0.3796)	(+26.08)	(−11.01)
$(CH_3)_2Pb$:	+36.49	−1.842	+37.04	−0.4211
	(+36.96)	(−0.3859)	(+37.27)	(−1.228)

[a] At the CCSD(T)/LANL2DZdp//B3LYP/LANL2DZ (B3LYP/LANL2DZ) levels of theory. For B3LYP-optimized structures of the stationary points, see Figure 3. [b] Energies differences have been zero-point-corrected. See text. [c] Energy relative to the corresponding singlet state. A positive value means the singlet is the ground state. [d] Stabilization energy of the precursor complex, relative to the corresponding reactants. [e] Activation energy of the transition state, relative to the corresponding reactants. [f] Reaction enthalpy of the product, relative to the corresponding reactants.

is in the order C < Si < Ge < Sn < Pb, the barrier height (kcal mol^{-1}) for SiH_4 activation increases in the order: Me_2C-TS (+1.5) < Me_2Si-TS (+6.3) < Me_2Ge-TS (+15) < Me_2Sn-TS (+25) < Me_2Pb-TS (+37). Likewise, the order of enthalpy (kcal mol^{-1}) follows the same trend as the activation energy: Me_2C-Pro (−86) < Me_2Si-Pro (−52) < Me_2Ge-Pro (−35) < Me_2Sn-Pro (−11) < Me_2Pb-Pro (−0.42). Again, the theoretical findings are in excellent agreement with the CM model. This investigation provides strong evidence that the singlet–triplet splitting can be used as a guide to predict the reactivity of the Me_2X species. Additionally, the computational results suggest that the barrier heights for insertion of dimethyl-substituted stannylene and plumbylene into SiH_4 are much larger than for the other three divalent species, while the reaction enthalpies of the former reactions are also much less exothermic than the latter. All of these computational results indicate that Me_2Ge, Me_2Sn, and Me_2Pb should be unreactive towards insertion into the Si–H bond. On the other hand, both Me_2C and Me_2Si readily insert into the Si–H bond. These theoretical findings have been confirmed by experimental observations.[8,20,21]

Germane insertion reactions: The stationary points shown in **5** were located for each germane insertion reaction [Eq. (3)] at both the DFT and CCSD(T) levels of theory. The optimized geometries of the stationary points can be found in Figure 4. The relative energies for each insertion reaction are presented in Table 4. Several intriguing results are found in the figure and in the table.

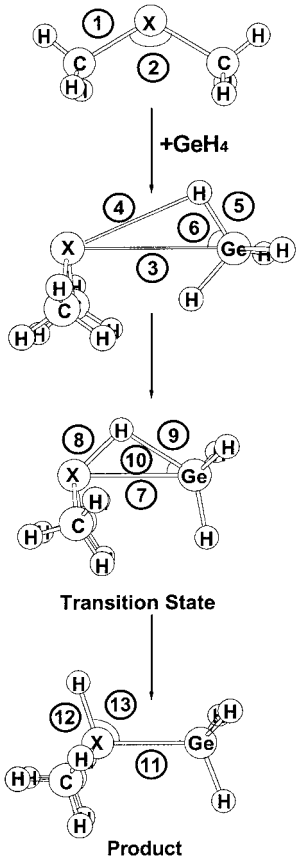

	C	Si	Ge	Sn	Pb
1	1.506	1.931	2.209	2.197	2.267
2	112.7	97.82	95.62	93.58	93.02
3	3.503	4.936	5.102	5.475	4.280
4	3.337	4.443	4.507	4.847	3.044
5	1.541	1.543	1.544	1.544	1.553
6	71.03	62.64	59.06	58.40	30.42
7	3.613	2.918	2.908	3.027	3.010
8	2.107	1.564	1.605	1.762	1.780
9	1.565	1.960	2.085	2.218	2.429
10	11.91	29.95	32.49	35.15	36.26
11	1.990	2.420	2.482	2.659	2.694
12	1.101	1.492	1.554	1.724	1.756
13	106.5	107.6	108.0	108.2	108.5

Figure 4. B3LYP/LANL2DZ-optimized geometries [Å, °] of the reactants (singlet), precursor complexes, transition states, and insertion products of $(CH_3)_2X$ (X = C, Si, Ge, Sn, Pb) and GeH_4

Table 4. Relative energies for singlet and triplet carbenes ($(CH_3)_2X$) and for the process: reactants ($(CH_3)_2X + GeH_4$)→precursor complex→transition state→insertion product.[a,b]

Systems	ΔE_{st}[c] [kcal mol^{-1}]	ΔE_{cpx}[d] [kcal mol^{-1}]	$\Delta E^{\neq}$[e] [kcal mol^{-1}]	ΔH[f] [kcal mol^{-1}]
$(CH_3)_2C$:	−0.4651	−1.962	+0.2355	−86.12
	(−4.951)	(−1.017)	(+1.054)	(−87.67)
$(CH_3)_2Si$:	+22.00	−0.7753	+1.492	−53.96
	(+21.59)	(−0.6275)	(+6.091)	(−48.48)
$(CH_3)_2Ge$:	+26.91	−0.8507	+9.330	−38.02
	(+27.64)	(−0.1443)	(+12.39)	(−36.12)
$(CH_3)_2Sn$:	+27.93	−0.7187	+18.72	−14.72
	(+29.36)	(−0.2259)	(+21.15)	(−13.81)
$(CH_3)_2Pb$:	+36.49	−1.483	+30.68	−4.817
	(+36.96)	(−0.2560)	(+32.25)	(−4.493)

[a] At the CCSD(T)/LANL2DZdp//B3LYP/LANL2DZ (B3LYP/LANL2DZ) levels of theory. For B3LYP-optimized structures of the stationary points, see Figure 4. [b] Energy differences have been zero-point-corrected. See text. [c] Energy relative to the corresponding singlet state. A positive value means the singlet is the ground state. [d] Stabilization energy of the precursor complex, relative to the corresponding reactants. [e] Activation energy of the transition state, relative to the corresponding reactants. [f] Reaction enthalpy of the product, relative to the corresponding reactants.

As in the methane and silane insertion reactions, all five transition state structures show the same three-center pattern involving X (X = C, Si, Ge, Sn, Pb), germanium, and hydrogen atoms. The main components of the transition vector correspond to displacement of Me_2X towards GeH_4, whose eigenvalue gives an imaginary frequency of $52.9i$ cm^{-1} for Me_2C-TS, $685i$ cm^{-1} for Me_2Si-TS, $724i$ cm^{-1} for Me_2Ge-TS, $725i$ cm^{-1} for Me_2Sn-TS, and $641i$ cm^{-1} for Me_2Pb-TS. As already discussed, the CCSD(T) calculations suggest increasing ΔE_{st} in the series $Me_2C < Me_2Si < Me_2Ge < Me_2Sn < Me_2Pb$. These results are in accordance with the trend in activation energy and enthalpy ($\Delta E^{\neq}$, ΔH): Me_2C (0.24, −86) < Me_2Si (1.5, −54) < Me_2Ge (9.3, −38) < Me_2Sn (19, −11) < Me_2Pb (31, −4.8) kcal mol^{-1} (Table 4). Again, the theoretical findings are in excellent agreement with the CM model. Thus, to find a good model for a facile germane insertion reaction, an understanding of the singlet–triplet splitting ΔE_{st} of the heavy carbene is crucial. Besides this, considering both the activation barrier and the reaction enthalpy obtained from the model calculations presented here, it is concluded that the greater the atomic number of the X center, the larger the activation energy, the less exothermic the insertion reaction, and therefore the more difficult is its insertion into the Ge–H bond of germane. These theoretical investigations are in agreement with some available experimental findings, especially for the germylene[20,22] and stannylene cases.[8]

Methanol insertion reactions: The reaction of Me_2X with n-type lone pair donors such as MeOH was also studied in this work. Selected geometrical parameters of reactants (Me_2X + MeOH), precursor complex, TS, and insertion product for Equation (4) are collected in Figure 5. The rela-

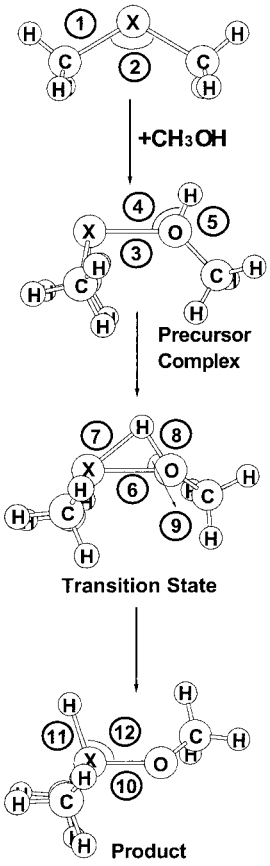

	C	Si	Ge	Sn	Pb
1	1.506	1.931	2.209	2.197	2.267
2	112.7	97.82	95.62	93.58	93.02
3	2.772	2.061	2.189	2.325	2.463
4	110.8	112.0	113.3	116.4	117.2
5	1.017	0.976	0.976	0.977	0.977
6	1.978	1.977	2.053	2.125	2.194
7	2.159	1.690	1.698	1.849	1.831
8	0.977	1.271	1.359	1.428	1.543
9	86.96	57.95	55.29	58.88	55.40
10	1.470	1.717	1.805	1.939	2.024
11	1.106	1.498	1.558	1.729	1.761
12	108.3	108.6	108.1	108.3	106.7

Figure 5. B3LYP/LANL2DZ-optimized geometries [Å, °] of the reactants (singlet), precursor complexes, transition states, and insertion products of $(CH_3)_2X$ (X = C, Si, Ge, Sn, Pb) and CH_3OH.

tive energies of these stationary points are summarized in Table 5. Several interesting conclusions can be drawn from Table 5 and Figure 5.

Table 5. Relative energies for singlet and triplet carbenes ($(CH_3)_2X$) and for the process: reactants ($(CH_3)_2X + CH_3OH$)precursor complex→transition state→insertion product.[a,b]

System	ΔE_{st}[c] [kcal mol^{-1}]	ΔE_{cpx}[d] [kcal mol^{-1}]	ΔE^{+}[e] [kcal mol^{-1}]	ΔH[f] [kcal mol^{-1}]
$(CH_3)_2C$:	−0.4651	−6.707	−1.526	−81.91
	(−4.951)	(−1.694)	(−3.556)	(−83.87)
$(CH_3)_2Si$:	+22.00	−9.947	+5.092	−72.10
	(+21.59)	(−14.74)	(+1.997)	(−64.82)
$(CH_3)_2Ge$:	+26.91	−7.737	+15.41	−46.02
	(+27.64)	(−14.20)	(+9.623)	(−46.79)
$(CH_3)_2Sn$:	+27.93	−10.25	+23.75	−29.15
	(+29.36)	(−14.94)	(+15.14)	(−33.96)
$(CH_3)_2Pb$:	+36.49	−9.581	+37.76	−1.822
	(+36.96)	(−12.27)	(+29.43)	(−6.536)

[a] At the CCSD(T)/LANL2DZdp//B3LYP/LANL2DZ (B3LYP/LANL2DZ) levels of theory. For B3LYP-optimized structures of the stationary points, see Figure 5. [b] Energies differences have been zero-point-corrected. See text. [c] Energy relative to the corresponding singlet state. A positive value means the singlet is the ground state. [d] Stabilization energy of the precursor complex, relative to the corresponding reactants. [e] Activation energy of the transition state, relative to the corresponding reactants. [f] Reaction enthalpy of the product, relative to the corresponding reactants.

First, the closed-shell Me_2X electron configuration is such that there is a vacant p orbital on X capable of forming chemical bonds with a Lewis base such as ammonia, water, or hygrogen fluoride. As can be seen in Figure 5, these precursor complexes ($Me_2X\cdots MeOH$) appear to have the same structure, in which optimal overlap between the lone pair orbital of MeOH and the empty p orbital of Me_2X is achieved by an orthogonally planar approach of the two molecules (see Scheme 2). The donor–acceptor interaction leads to calculated C–O, Si–O, Ge–O, Sn–O, and Pb–O bond lengths of 1.93, 2.06, 2.19, 2.33, and 2.46 Å, respectively. Attempts to locate molecular complexes at much longer X–O distances failed. Thus, the theoretical findings suggest that the complexes obtained in this work can be considered as Lewis acid–base adducts.

Scheme 2.

Furthermore, an intriguing question here is whether the initial formation of the donor–acceptor complex from $Me_2X + MeOH$ is reversible. In principle, it is the depth of the well for the precursor complex that determines whether the barrier lies above or below the reactant threshold. Deepening the well of the molecular complex may lower the barrier to reaction below the energy of the reactants. For instance, as shown in Table 5, in the $Me_2C + MeOH$ case, the energy of the transition state is below the energy of the reactants, so that no net barrier to reaction exists. The present theoretical findings indicate that the formation of the $Me_2C\cdots MeOH$ Lewis acid–base adduct should not be reversible. On the other hand, as seen in Table 5, the stabilization energies of the other four precursor complexes (PC) are large, for example, Me_2Si-PC (−9.9 kcal mol^{-1}), Me_2Ge-PC (−7.7 kcal mol^{-1}), Me_2Sn-PC (−10 kcal mol^{-1}), and Me_2Pb-PC (−9.6 kcal mol^{-1}). Additionally, the energy of the transition states relative to their corresponding reactants are Me_2Si-TS (+5.1 kcal mol^{-1}), Me_2Ge-TS (+15 kcal mol^{-1}), Me_2Sn-TS (+24 kcal mol^{-1}), and Me_2Pb-TS (+38 kcal mol^{-1}); that is, the $Me_2X + MeOH$ (X = Si, Ge, Sn, and Pb) reactions may not have enough energy to overcome the barrier to insertion, and their donor–acceptor complexes ($Me_2X\cdots MeOH$) should exist as local minima. All of the theoretical evidence suggests that the overall reactions of $Me_2X + MeOH$ should not be reversible. Indeed, to my knowledge, no experimental evidence of reversibility in $Me_2X + MeOH$ reactions at room temperature has been reported.[8,23,24]

Second, the DFT frequency calculations for the transition states Me_2C-TS, Me_2Si-TS, Me_2Ge-TS, Me_2Sn-TS, and Me_2Pb-TS showed that the single imaginary frequency values are 58.0*i*, 1360*i*, 1332*i*, 1281*i*, and 1183*i* cm^{-1}, respectively. As mentioned above, the primary similarity between the optimized transition states of Equation (4) was a structure of C_1 symmetry resembling a Lewis acid–base adduct.

As shown in Table 5, the CCSD(T) barrier heights (kcal mol^{-1}) for the insertion reactions increase in the order: Me_2C-TS (−2.2) < Me_2Si-TS (+5.1) < Me_2Ge-TS (+15) < Me_2Sn-TS (+24) < Me_2Pb-TS (+38). Also, their reaction enthalpies (kcal mol^{-1}) increase in the order: Me_2C (−82) < Me_2Si (−72) < Me_2Ge (−46) < Me_2Sn (−29) < Me_2C (−1.8). Again, one can easily observe that both orders follow the same trend as the singlet–triplet splitting ΔE_{st} of Me_2X, as shown above. This strongly implies that the values of ΔE_{st} are remarkably diagnostic of the reactivities of heavy carbene species.[14,15] Finally, the present theoretical investigations predicted that Me_2C, Me_2Si, Me_2Ge, and Me_2Sn should insert readily into the O–H bond of MeOH at room temperature, which has been confirmed by some available experimental observations.[8,24] Nevertheless, the calculations also imply that Me_2Pb insertion into the MeOH molecule is nearly thermoneutral, with an exothermicity of less than 2 kcal mol^{-1}. Hence, Me_2Pb should not insert readily into the O–H bond. As there are no relevant experimental and theoretical data on such systems, the above result is a prediction.

Ethane insertion reactions: The reaction of Me_2X with C_2H_6 was studied in the present work. Selected geometrical parameters of reactants ($Me_2X + C_2H_6$), precursor complex, TS, and insertion product for Equation (5) are shown in Figure 6. The relative energies of these stationary points are summarized in Table 6. The major conclusions that can be drawn from Table 6 and Figure 6 follow.

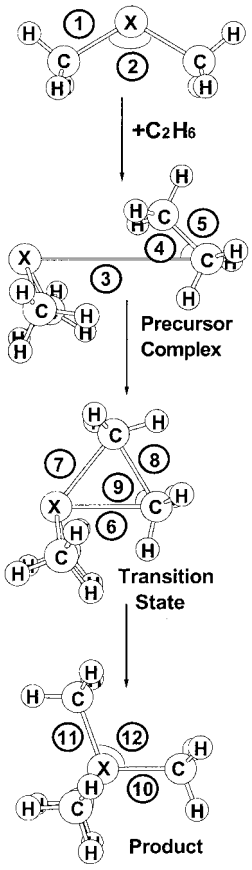

	C	Si	Ge	Sn	Pb
1	1.506	1.931	2.209	2.197	2.267
2	112.7	97.82	95.62	93.58	93.02
3	4.046	4.619	4.455	4.606	5.425
4	68.43	66.33	46.38	55.72	65.90
5	1.544	1.543	1.543	1.542	1.543
6	2.233	2.473	2.529	2.654	2.714
7	2.001	2.293	2.340	2.490	2.535
8	1.894	2.084	2.170	2.255	2.365
9	57.30	59.70	59.15	60.31	59.40
10	1.551	1.902	1.977	2.148	2.206
11	1.550	1.902	1.977	2.148	2.206
12	109.5	109.5	109.6	109.7	110.0

Figure 6. B3LYP/LANL2DZ-optimized geometries [Å, °] of the reactants (singlet), precursor complexes, transition states, and insertion products of $(CH_3)_2X$ (X = C, Si, Ge, Sn, Pb) and C_2H_6.

Table 6. Relative energies for singlet and triplet carbenes ($(CH_3)_2X$) and for the process: reactants ($(CH_3)_2X + C_2H_6$)→precursor complex→transition state→insertion product.[a,b]

System	ΔE_{st}[c] [kcal mol^{-1}]	ΔE_{cpx}[d] [kcal mol^{-1}]	$\Delta E^{\neq}$[e] [kcal mol^{-1}]	ΔH[f] [kcal mol^{-1}]
$(CH_3)_2C$:	−0.4651	−1.182	+55.02	−74.00
	(−4.951)	(−0.2209)	(+57.61)	(−85.25)
$(CH_3)_2Si$:	+22.00	−1.326	+58.76	−62.42
	(+21.59)	(−0.3640)	(+60.91)	(−58.34)
$(CH_3)_2Ge$:	+26.91	−2.103	+62.80	−39.62
	(+27.64)	(−0.3721)	(+63.22)	(−41.25)
$(CH_3)_2Sn$:	+27.93	−1.800	+66.57	−20.49
	(+29.36)	(−0.4675)	(+66.35)	(−25.29)
$(CH_3)_2Pb$:	+36.49	−1.852	+71.43	−14.39
	(+36.96)	(−0.1763)	(+72.25)	(−17.45)

[a] At the CCSD(T)/LANL2DZdp//B3LYP/LANL2DZ (B3LYP/LANL2DZ) levels of theory. For B3LYP-optimized structures of the stationary points, see Figure 6. [b] Energy differences have been zero-point-corrected. See text. [c] Energy relative to the corresponding singlet state. A positive value means the singlet is the ground state. [d] Stabilization energy of the precursor complex, relative to the corresponding reactants. [e] Activation energy of the transition state, relative to the corresponding reactants. [f] Reaction enthalpy of the product, relative to the corresponding reactants.

Like the case of methane insertion shown previously, my computational results indicate that singlet-state Me_2X inserts into the C–C bond of C_2H_6 in a concerted manner via a three-center transition state, and that the stereochemistry at the X center (X = C, Si, Ge, Sn, Pb) is preserved. The B3LYP/LANL2DZ frequency calculations for the transition states Me_2C-TS, Me_2Si-TS, Me_2Ge-TS, Me_2Sn-TS, and Me_2Pb-TS gave single imaginary frequency values of 831*i*, 700*i*, 612*i*, 569*i*, and 480*i* cm^{-1}, respectively. Again, as demonstrated in Table 6, it can be seen that the trend in ΔE_{st} of Me_2X is in reasonable agreement with the that in the activation energies (kcal mol^{-1}): Me_2C-TS (+55) < Me_2Si-TS (+59) < Me_2Ge-TS (+63) < Me_2Sn-TS (+67) < Me_2Pb-TS (+71). Moreover, all the C–C bond insertion reactions are thermodynamically exothermic. The order of exothermicity also follows the same trend as that of the ΔE_{st} of Me_2X (kcal mol^{-1}): Me_2C-Pro (−74) < Me_2Si-Pro (−62) < Me_2Ge-Pro (−40) < Me_2Sn-Pro (−20) < Me_2Pb-Pro (−14). Again, these phenomena emphasize that the singlet–triplet splitting ΔE_{st} of Me_2X plays a key role in determining its chemical reactivity. Furthermore, the calculated barrier heights are quite sizable (55–71 kcal mol^{-1}), and this suggests that dimethyl-substituted heavy carbenes are kinetically stable with respect to insertion into the C–C bond of alkanes. Indeed, my theoretical results are consistent with some experimental evidence that Me_2Sn does not insert readily into the C–C bond.[8]

Ethene cycloaddition reactions: In this section the results for the four regions on the potential energy surfaces of **5** are presented: the reactants ($Me_2X + C_2H_4$), the precursor complex, the TS, and the cycloaddition product [see Eq. (6)]. The fully optimized geometries for these stationary points, calculated at the B3LYP/LANL2DZ level, are given in

Figure 7. The relative energies at the DFT and CCSD(T) levels of theory are collected in Table 7. Several interesting results obtained from Figure 7 and Table 7 follow.

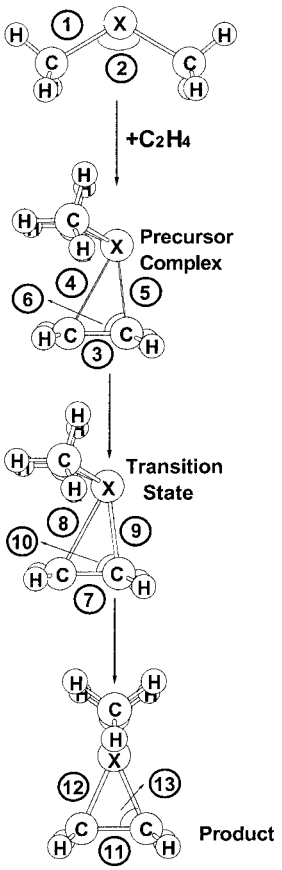

	C	Si	Ge	Sn	Pb
1	1.506	1.931	2.209	2.197	2.267
2	112.7	97.82	95.62	93.58	93.02
3	1.350	1.350	1.415	1.368	1.359
4	3.835	4.263	3.459	2.944	3.087
5	3.227	3.743	2.874	2.725	2.960
6	106.5	103.4	83.66	85.15	82.31
7	1.353	1.354	1.422	1.476	1.543
8	3.272	3.046	2.418	2.319	2.237
9	2.774	2.337	2.145	2.209	2.197
10	99.06	90.25	82.66	75.07	71.00
11	1.541	1.576	1.573	1.567	1.584
12	1.533	1.883	1.965	2.138	2.195
13	59.84	65.25	66.41	68.52	69.17

Figure 7. B3LYP/LANL2DZ-optimized geometries [Å, °] of the reactants (singlet), precursor complexes, transition states, and insertion products of $(CH_3)_2X$ (X = C, Si, Ge, Sn, Pb) and C_2H_4.

Table 7. Relative energies for singlet and triplet carbenes ($(CH_3)_2X$) and for the process: reactants ($(CH_3)_2X+C_2H_4$)→precursor complex→transition state→addition product.[a,b]

System	ΔE_{st}[c] [kcal mol^{-1}]	ΔE_{cpx}[d] [kcal mol^{-1}]	$\Delta E^{\neq}$[e] [kcal mol^{-1}]	ΔH[f] [kcal mol^{-1}]
$(CH_3)_2C$:	−0.4651	−0.9522	−??7290	−83.31
	(−4.951)	(−0.1883)	(+0.8120)	(−78.91)
$(CH_3)_2Si$:	+22.00	−3.754	−2.026	−43.58
	(+21.59)	(−0.8842)	(−1.034)	(−36.65)
$(CH_3)_2Ge$:	+26.91	−6.306	−3.487	−19.49
	(+27.64)	(−5.041)	(−5.063)	(−17.73)
$(CH_3)_2Sn$:	+27.93	−5.066	+4.098	+0.2681
	(+29.36)	(−4.121)	(+3.585)	(−0.6903)
$(CH_3)_2Pb$:	+36.49	−5.457	+24.40	+24.41
	(+36.96)	(−3.540)	(+24.32)	(+24.33)

[a] At the CCSD(T)/LANL2DZdp//B3LYP/LANL2DZ (B3LYP/LANL2DZ) levels of theory. For B3LYP-optimized structures of the stationary points, see Figure 7. [b] Energies differences have been zero-point-corrected. See text. [c] Energy relative to the corresponding singlet state. A positive value means the singlet is the ground state. [d] Stabilization energy of the precursor complex, relative to the corresponding reactants. [e] Activation energy of the transition state, relative to the corresponding reactants. [f] Reaction enthalpy of the product, relative to the corresponding reactants.

Since the Me_2X plus ethene reaction leads to a three-membered cyclic product, as expected for a 1,2-addition, it is reasonable to assume a parallel planar approach of Me_2X to ethylene in the formation of the π complex.[11c] As can be seen in Figure 7, the parallel planar orientation of the reacting molecules is maintained along this reaction coordinate. The transition state for each Me_2X addition reaction was located at the B3LYP/LANL2DZ level of theory. The optimized geometries of the five transition states can be found in Figure 7. Examination of the single imaginary frequency for each transition state (56.8i cm^{-1} for Me_2C-TS, 41.5i cm^{-1} for Me_2Si-TS, 58.1i cm^{-1} for Me_2Ge-TS, 150i cm^{-1} for Me_2Sn-TS, and 75.0i cm^{-1} for Me_2Pb-TS) provides excellent confirmation of the concept of a cycloaddition process. Moreover, the energy of the transition state relative to its corresponding precursor complex, at the CCSD(T) level, is calculated to increase in the order (kcal mol^{-1}): Me_2C-TS (+0.22) < Me_2Si-TS (+1.7) < Me_2Ge-TS (+2.8) < Me_2Sn-TS (+9.1) < Me_2Pb-TS (+30). The trend in reaction enthalpy also mirrors the trend in activation energy: Me_2C-Pro (−83) < Me_2Si-Pro (−44) < Me_2Ge-Pro (−19) < Me_2Sn-Pro (+0.27) < Me_2Pb-Pro (+24). Again, these trends reflect that of ΔE_{st}, which increases as X changes from C to Pb. These results are also consistent with the prediction that the activation barrier should be correlated to the reaction enthalpy for a cycloaddition.[14,15] Finally, the energies of the cycloaddition products for both Me_2Sn and Me_2Pb are above those of the corresponding reactants. This strongly implies that the cycloaddition reactions of stannylene and plumbylene to alkenes should be energetically unfavorable from a thermodynamic viewpoint. This is in good agreement with the experimental observation that Me_2Sn is unreactive towards alkenes.[8]

Ethyne cycloaddition reactions: The fully optimized geometries of the reactants, the precursor complex, the TS, and the ethyne cycloaddition product [Eq. (7)] for Me_2X calculated at the B3LYP/LANL2DZ level are collected in Figure 8. Their relative energies at the DFT and CCSD(T) levels of theory are summarized in Table 8. The major conclusions that can be drawn from Table 8 and Figure 8 are discussed below.

As in the case of ethylene cycloaddition to Me_2X, model systems showed that ethyne cycloaddition reactions all proceed in a concerted fashion via a three-center transition state in the π-attack pathway,[11c] as shown in Figure 8. These transition structures are characterized by one imaginary frequency of 180i, 121i, 137i, 184i, and 75.0i cm^{-1} for Me_2C-TS, Me_2Si-TS, Me_2Ge-TS, Me_2Sn-TS, and Me_2Pb-TS, respectively. The normal coordinate corresponding to the imaginary frequency is primarily the motion of the Me_2X species toward the C≡C triple bond, as found in the TS for ethylene cycloaddition to Me_2X. As demonstrated in Table 8, the trends in ΔE_{st} of Me_2X correlate well with those in activation energy and enthalpy ($\Delta E^{\neq}$, ΔH) for the cycloaddition reaction: Me_2C (+0.12, −72) < Me_2Si (−1.9, −51) < Me_2Ge (−4.0, −27) < Me_2Sn (+2.4, −8.4) < Me_2Pb (+18, +17) kcal mol^{-1}. Again, all of the theoretical observations strongly suggest that the singlet–triplet separation ΔE_{st} of Me_2X plays a decisive role in determining the chemical reac-

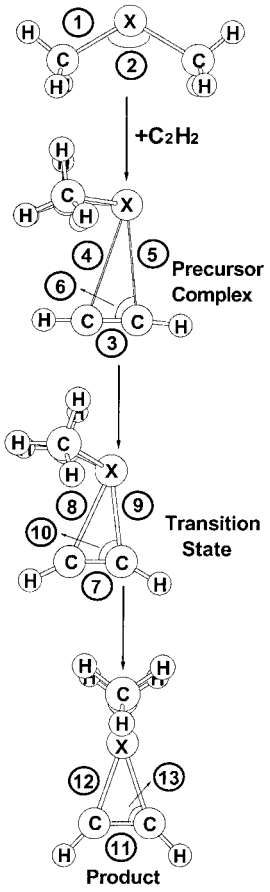

	C	Si	Ge	Sn	Pb
1	1.506	1.931	2.209	2.197	2.267
2	112.7	97.82	95.62	93.58	93.02
3	3.503	4.936	5.102	5.475	4.280
4	3.337	4.443	4.507	4.847	3.044
5	1.541	1.543	1.544	1.544	1.553
6	71.03	62.64	59.06	58.40	30.42
7	3.613	2.918	2.908	3.027	3.010
8	2.107	1.564	1.605	1.762	1.780
9	1.565	1.960	2.085	2.218	2.429
10	11.91	29.95	32.49	35.15	36.26
11	1.990	2.420	2.482	2.659	2.694
12	1.101	1.492	1.554	1.724	1.756
13	106.5	107.6	108.0	108.2	108.5

Figure 8. B3LYP/LANL2DZ-optimized geometries [Å, °] of the reactants (singlet), precursor complexes, transition states, and insertion products of $(CH_3)_2X$ (X = C, Si, Ge, Sn, Pb) and C_2H_2.

Table 8. Relative energies for singlet and triplet carbenes ($(CH_3)_2X$) and for the process: reactants ($(CH_3)_2X + C_2H_2$)→precursor complex→transition state→addition product.[a,b]

Systems	ΔE_{st}[c] [kcal mol^{-1}]	ΔE_{cpx}[d] [kcal mol^{-1}]	$\Delta E^{\neq}$[e] [kcal mol^{-1}]	ΔH[f] [kcal mol^{-1}]
$(CH_3)_2C$:	−0.4651	−3.180	+0.1216	−71.69
	(−4.951)	(−0.8321)	(+0.7850)	(−67.35)
$(CH_3)_2Si$:	+22.00	−4.396	−1.854	−51.45
	(+21.59)	(−2.225)	(−1.249)	(−41.70)
$(CH_3)_2Ge$:	+26.91	−1.176	−4.029	−26.74
	(+27.64)	(−1.391)	(−3.672)	(−23.03)
$(CH_3)_2Sn$:	+27.93	−4.767	+2.420	−8.395
	(+29.36)	(−3.324)	(+1.202)	(−8.362)
$(CH_3)_2Pb$:	+36.49	−4.994	+18.14	+17.56
	(+36.96)	(−3.065)	(+17.63)	(+17.69)

[a] At the CCSD(T)/LANL2DZdp//B3LYP/LANL2DZ (B3LYP/LANL2DZ) levels of theory. For B3LYP-optimized structures of the stationary points, see Figure 8. [b] Energy differences have been zero-point-corrected. See text. [c] Energy relative to the corresponding singlet state. A positive value means the singlet is the ground state. [d] Stabilization energy of the precursor complex, relative to the corresponding reactants. [e] Activation energy of the transition state, relative to the corresponding reactants. [f] Reaction enthalpy of the product, relative to the corresponding reactants.

tivity of the heavy carbene species. Furthermore, it is noteworthy that the CCSD(T) results show that the activation energy for the cycloaddition of Me_2Sn to C_2H_2 is quite small, just above the energy of the reactants by 2.4 kcal mol^{-1}. On the other hand, the exothermicity of the reaction is predicted to be −8.4 kcal mol^{-1}. These theoretical results suggest that Me_2Sn should be reactive towards ethyne, which has been confirmed by Walsh et al.[8] Nevertheless, our theoretical investigations also predict that Me_2Pb should be unreactive towards alkynes. Since there are no relevant experimental and theoretical data on this system, this result can be regarded as a prediction.

Conclusion

As the above analysis has demonstrated, the CM approach adds additional facets and insights into this relatively poorly understood area of mechanistic studies for both stannylenes and plumbylenes. Although the relative reactivity of heavy carbenes is determined by the entire potential energy surface, the concepts of the CM model, which focuses on the singlet–triplet splitting in the reactants, allows one to assess quickly the relative reactivity of a variety of heavy carbenes without specific knowledge of the actual energies of the interactions involved. Therefore, the energetic separation between the lowest singlet and triplet electronic states of a heavy carbene is perhaps the most critical parameter required for the prediction of the reactivity of these fascinating species. In spite of its simplicity, my approach can provide chemists with important insights into the factors controlling the activation energies for both insertion and addition reactions, and thus permit them to predict the reactivity of unknown substituted heavy carbenes. The predictions may be useful as a guide to future synthetic efforts and to indicate problems that merit further study by both theory and experiment. It is hoped that the present work will stimulate a further research into this subject.

Methods of Calculation

All geometries were fully optimized without imposing any symmetry constraints, although in some instances the resulting structure showed various elements of symmetry. Their geometries and energetics were calculated by using nonlocalized DFT in conjunction with a standard LANL2DZ basis set,[25] which is denoted as B3LYP/LANL2DZ.[26] The spin-unrestricted (UB3LYP) formalism was used for the open-shell (triplet) species. Frequency calculations were performed on all structures to confirm that the reactants, intermediates, and products had no imaginary frequencies, and that transition states possessed only one imaginary frequency. The relative energies were thus corrected for vibrational zero-point energies (ZPE, not scaled).

Single-point energies were also calculated at CCSD(T)(frozen)/LANL2DZdp//B3LYP/LANL2DZ level of theory,[27] to improve the treatment of electron correlation. Unless otherwise noted, relative energies given in the text are those determined at the CCSD(T) level[28] and include vibrational zero-point energy (ΔZPE) corrections determined at the B3LYP/LANL2DZ level. Furthermore, seven of the reactions that we have investigated [i.e., Me_2C in Eqs. (1)–(7)] were probed in some detail by determining the intrinsic reaction coordinate (IRC) with the algorithm proposed by Schlegel.[29]

In any event, our IRC calculations show that the transition states we found in this work should be true transition states since they correctly link either the reactants or the precursor complexes. All calculations were performed with the Gaussian 98/DFT package.[30,31]

Acknowledgement

I am grateful to the National Center for High-Performance Computing of Taiwan for generous amounts of computing time and the National Science Council of Taiwan for financial support. Special thanks are also due to the referees for very helpful suggestions and comments.

[1] a) R. A. Abramovitch in *Reactive Intermediates*, *Vol. 1* (Ed.: R. A. Moss), Plenum, New York, **1980**, p. 218; b) R. A. Moss, M. Jones, Jr. in *Reactive Intermediates*, *Vol. 3*, Wiley, New York, **1985**, Chap. 3; c) M. S. Platz in *Kinetics and Spectroscopy of Carbenes and Biradicals*, Plenum, New York, **1990**; d) H. Tomioka, *Res. Chem. Intermed.* **1994**, *20*, 605; e) M. Driess, H. Grutzmacher, *Angew. Chem.* **1996**, *108*, 900; *Angew. Chem. Int. Ed. Engl.* **1996**, *35*, 829; and references therein.

[2] a) J. M. Jasinski, B. S. Meyerson, B. A. Scott, *Annu. Rev. Phys. Chem.* **1987**, *38*, 109; b) P. P. Gaspar in *Reactive Intermediates,Vol. 1* (Eds.: M. Jones, Jr., R. A. Moss), Wiley, New York, **1978**, p. 229; c) R. West, T. J. Barton, *J. Chem. Educ.* **1980**, *57*, 165; d) R. West, T. J. Barton, *J. Chem. Educ.* **1980**, *57*, 335.

[3] a) M. Lesbre, P. Mazerroles, J. Satgé, *The Organic Compounds of Germanium*, Zinatne, Riga, **1990**; b) E. Lukevics, T. Gar, L. Ignatovich, B. Mironov, *Biological Activity of Germanium*, Zinatne, Riga, **1993**; c) E. Lukevics, L. Ignatovich, *Frontiers of Organogermanium-Tin-Lead Chemistry*, Latvian Institute, Riga, **1993**; d) S. Patai, *The Chemistry of Organic Germanium, Tin, and Lead Compounds*, Wiley, New York, **1995**; e) P. Riviere, M. Riviere-Baudet, J. Satgé in *Comprehensive Organometallic Chemistry*, *Vol. 2* (Eds.: G. Wilkinson, F. G. A. Stone, E. W. Abel), Pergamon, Oxford, **1982**, Chap. 10; f) P. Riviere, M. Riviere-Baudet, J. Satgé in *Comprehensive Organometallic Chemistry Vol. 2*, (Eds.: E. W. Abel, F. G. A. Stone, G. Wilkinson), Pergamon, Oxford, **1995**, Chap. 5; g) P. Riviere, M. Riviere-Baudet, J. Satgé in in *Comprehensive Organometallic Chemistry Vol. 2*, (Eds.: E. W. Abel, F. G. A. Stone, G. Wilkinson), Pergamon, Oxford, **1982**, Chap. 10; h) P. Riviere, M. Riviere-Baudet, J. Satgé in *Comprehensive Organometallic Chemistry Vol. 2*, (Eds.: E. W. Abel, F. G. A. Stone, G. Wilkinson), Pergamon, Oxford, **1995**, Chap. 5.

[4] a) J. W. Connolly, C. Hoff, *Adv. Organomet. Chem.* **1981**, *19*, 123; b) M. Veith, O. Recktenwald, *Top. Curr. Chem.* **1982**, *104*, 1; c) W. P. Neumann, *Chem. Rev.* **1991**, *91*, 311; d) M. F. Lappert, *Main Group Met. Chem.* **1994**, *17*, 183; e) A. Asadi, C. Eaborn, M. S. Hill, P. B. Hitchcock, M. M. Meehan, J D. Smith, *Organometallics* **2002**, *21*, 2430.

[5] The ability of R ligands to bond to the tin center is often ambivalent: they can act as donors (through their filled 5σ orbital) or as acceptors through their empty 5p orbitals) towards a transition metal center: a) P. J. Davidson, M. F. Lappert, *J. Chem. Soc. Chem. Commun.* **1973**, 317; b) J. D. Cotton, P. J. Davidson, D. E. Goldberg, M. F. Lappert, K. M. Thomas, *J. Chem. Soc. Chem. Commun.* **1974**, 893; c) M. Veith, *Angew. Chem.* **1975**, *87*, 287; *Angew. Chem. Int. Ed. Engl.* **1975**, *14*, 263; d) D. H. Harris, M. F. Lappert, J. B. Pedley, G. J. Sharp, *J. Chem. Soc. Dalton Trans.* **1976**, 945; e) P. J. Davidson, D. H. Harris, M. F. Lappert, *J. Chem. Soc. Dalton Trans.* **1976**, 2268; f) J. D. Cotton, P. J. Davidson, M. F. Lappert, *J. Chem. Soc. Dalton Trans.* **1976**, 2275; g) M. Veith, *Z. Naturforsch. B* **1978**, *33*, 7; h) P. B. Hitchcock, M. F. Lappert, S. A. Thomas, A. J. Thorne, *J. Organomet. Chem.* **1986**, *315*, 27; i) M. Kira, R. Yauchibara, R. Hirano, C. Kabuto, H. Sakurai, *J. Am. Chem. Soc.* **1991**, *113*, 7785; j) H. Grutzmacher, H. Pritzkow, F. T. Edelmann, *Organometallics* **1991**, *10*, 23; k) S. Brooker, J.-K. Buijink, F. T. Edelmann, *Organometallics* **1991**, *10*, 25; l) N. Tokitoh, M. Saito, R. Okazaki, *J. Am. Chem. Soc.* **1993**, *115*, 2065; m) M. Weidenbruch, A. Stilter, K. Peters, H. G. von Schnering, *Chem. Ber.* **1996**, *129*, 1565; n) K. W. Klinkhammer, T. F. Fassler, H. Grutzmacher, *Angew. Chem.* **1998**, *110*, 114–116; *Angew. Chem. Int. Ed. Engl.* **1998**, *37*, 124–126; o) U. Layh, H. Pritzkow, H. Grutzmacher, *J. Chem. Soc. Chem. Commun.* **1992**, 260; p) M. Weidenbruch, H. Kilian, K. Peters, H. G. von Schnering, H. Marsmann, *Chem. Ber.* **1995**, *128*, 983; q) A. Asadi, C. Eaborn, M. S. Hill, P. B. Hitchcock, M. M. Meehan, J. D. Smith, *Organometallics* **2002**, *21*, 2430.

[6] a) K. W. Klinkhammer, W. Schwarz, *Angew. Chem.* **1995**, *107*, 1448; *Angew. Chem. Int. Ed. Engl.* **1995**, *34*, 1334; b) M. Sturmann, W. Saak, K. W. Klinkhammer, M. Weidenbruch, *Z. Anorg. Allg. Chem.* **1999**, *625*, 1955; c) C. J. Cardin, D. J. Cardin, S. P. Constantine, A. K. Todd, S. J. Teat, S. Coles, *Organometallics* **1998**, *17*, 2144; d) S. Benet, C. J. Cardin, D. J. Cardin, S. P. Constantine, P. Heath, H. Rashid, S. Teixeira, J. H. Thorpe, A. K. Todd, *Organometallics* **1999**, *18*, 389; e) C. Drost, B. Gehrhus, P. B. Hitchcock, M. F. Lappert, *Chem. Commun.* **1997**, 1845; f) B. Gehrhus, P. B. Hitchcock, M. F. Lappert, *Angew. Chem.* **1997**, *109*, 2624–2626; *Angew. Chem. Int. Ed. Engl.* **1997**, *36*, 2514–2516; g) E. Eichler, P. P. Power, *Inorg. Chem.* **2000**, *39*, 5444; h) E. Eichler, B. L. Phillips, P. P. Power, *Inorg. Chem.* **2000**, *39*, 5450; i) W. Setaka, K. Sakamoto, M. Kira, P. P. Power, *Organometallics* **2001**, *20*, 4460.

[7] a) For example: K. Hillner, W. P. Neumann, *Tetrahedron Lett.* **1986**, *27*, 5347; b) C. Pluta, K. R. Porschke, R. Mynott, P. Betz, C. Kruger, *Chem. Ber.* **1991**, *124*, 1321; c) H. Grutzmacher, S. Freitag, R. Herbst-Irmer, G. S. Sheldrick, *Angew. Chem.* **1992**, *104*, 459; *Angew. Chem. Int. Ed. Engl.* **1992**, *31*, 437; d) J. Krause, C. Pluta, K. R. Porschke, R. Goddard, *J. Chem. Soc. Chem. Commun.* **1993**, 1254; e) J. Krause, K. H. Haack, K.-R. Porschke, B. Gabor, R. Goddard, C. Pluta, K. Seevogel, *J. Am. Chem. Soc.* **1996**, *118*, 804; f) F. Schager, K. Seevogel, K.-R. Porschke, M. Kessler, C. Kruger, *J. Am. Chem. Soc.* **1996**, *118*, 13075; g) P. Braunstein, V. Huch, C. Stern, M. Veith, *Chem. Commun.* **1996**, 2041; h) M. Veith, M. Olbrich, W. Shihua, V. Huch, *J. Chem. Soc. Dalton Trans.* **1996**, 161; i) J. J. Schneider, J. Hagen, D. Blaser, R. Boese, C. Kruger, *Angew. Chem.* **1997**, *109*, 739–742; *Angew. Chem. Int. Ed. Engl.* **1997**, *36*, 715–718; j) C. Drost, P. B. Hitchcock, M. F. Lappert, *Organometallics* **1998**, *17*, 3838; k) C. J. Carmalt, J. A. C. Clyburne, A. H. Cowley, V. Lomeli, B. G. McBurnett, *Chem. Commun.* **1998**, 243; l) J. J. Schneider, N. Czap, D. Blaser, R. Boese, *J. Am. Chem. Soc.* **1999**, *121*, 1409; m) J. J. Schneider, N. Czap, *J. Organomet. Chem.* **1999**, *584*, 338; n) J. J. Schneider, N. Czap, *J. Chem. Soc. Dalton Trans.* **1999**, 595; o) M. Veith, A. Rammo, S. Faber, B. Schillo, *Pure Appl. Chem.* **1999**, *71*, 401; p) B. Gehrhus, P. B. Hitchcock, M. F. Lappert, *J. Chem. Soc. Dalton Trans.* **2000**, 3094; q) C. Drost, P. B. Hitchcock, M. F. Lappert, *Organometallics* **2002**, *21*, 2095.

[8] R. Becerra, S. E. Boganov, M. P. Egorov, V. I. Faustov, I. V. Krylova, O. M. Nefedov, R. Walsh, *J. Am. Chem. Soc.* **2002**, *124*, 7555.

[9] a) W. Kirmse, *Carbene Chemistry*, 2nd ed., Academic Press, New York, **1971**; b) R. A. Moss, M. Jones, Jr., *Carbenes*, *Vol. 1*, Wiley, New York, **1973**; c) M. Jones, Jr., R. A. Moss, *Carbenes*, *Vol. 2*, Wiley, New York, **1975**; d) R. A. Moss, M. Jones, Jr., *Reactive Intermediates*, *Vol. 1*, Wiley, New York, **1978**; e) R. A. Moss, M. Jones Jr., *Reactive Intermediates*, *Vol. 2*, Wiley, New York, **1981**; f) R. A. Moss, M. Jones, Jr., *Reactive Intermediates*, *Vol. 3*, Wiley, New York, **1985**; g) R. A. Abramovitch, *Reactive Intermediates*, *Vol. 1*, Plenum, New York, **1980**; h) M. S. Platz, *Kinetics and Spectroscopy of Carbenes And Biradicals*, Plenum, New York, **1990**; i) R. A. Moss, *Acc. Chem. Res.* **1980**, *13*, 58; j) R. A. Moss, *Acc. Chem. Res.* **1989**, *22*, 15; k) M.-D. Su, *J. Phys. Chem.* **1996**, *100*, 4339, and references therein.

[10] a) P. P. Gaspar in *Reactive Intermediates*, *Vol. 2*, (Eds.: M. Jones, Jr., R. A. Moss) Wiley, New York, **1981**, p. 335; b) P. P. Gaspar in *Reactive Intermediates*, *Vol. 3* (Eds.: M. Jones, Jr., R. A. Moss), Wiley, New York, **1985**, p. 333; c) Y.-N. Tang in *Reactive Intermediates*, *Vol. 2* (Ed.: R. Abramowitch), Plenum Press, New York, **1982**, p. 297; d) P. P. Gaspar, D. Holten, S. Konieczny, J. Y. Corey, *Acc. Chem. Res.* **1987**, *20*, 329; e) J. M. Jasinski, R. Becerra, R. Walsh, *Chem. Rev.* **1995**, *95*, 1203; f) R. Becerra, R. Walsh in *Research in Chemical Kinetics*, *Vol. 3* (Eds.: R. G. Compton, G. Hancock), Elsevier Science, Amsterdam, **1995**; g) M.-D. Su, *J. Am. Chem. Soc.* **2002**, *124*, 12335, and references therein.

[11] a) M.-D. Su, S.-Y. Chu, *J. Phys. Chem. A* **1999**, *103*, 11011, and references therein; b) M.-D. Su, S.-Y. Chu, *J. Am. Chem. Soc.* **1999**, *121*, 4229, and references therein; c) M.-D Su, S.-Y. Chu, *J. Am. Chem. Soc.* **1999**, *121*, 11478, and references therein.

[12] a) M. Driess, R. Janoschek, H. Pritzkow, S. Rell, *Angew. Chem.* **1995**, *107*, 1746; *Angew. Chem. Int. Ed. Engl.* **1995**, *34*, 1614; b) K. Klinkhammer, *Polyhedron* **2002**, *21*, 587.

[13] a) M. J. S. Dewar, J. E. Friedheim, G. L. Grady, *Organometallics* **1985**, *4*, 1784; b) S. Sakai, *Int. Photogr. Int. J. Quant. Chem.* **1998**, *70*, 291.

[14] For details, see: a) S. Shaik, H. B. Schlegel, S. Wolfe in *Theoretical Aspects of Physical Organic Chemistry*, Wiley, New York, **1992**; b) A. Pross in *Theoretical and Physical Principles of Organic Reactivity*, Wiley, New York, **1995**; c) S. Shaik, *Prog. Phys. Org. Chem.* **1985**, *15*, 197.

[15] a) The first paper presenting the CM model: S. Shaik, *J. Am. Chem. Soc.* **1981**, *103*, 3692; b) Most up-to-date review of the CM model: S. Shaik, A. Shurki, *Angew. Chem.* **1999**, *111*, 616–657; *Angew. Chem. Int. Ed.* **1999**, *38*, 586–625.

[16] M.-D. Su, *Inorg. Chem.* **1995**, *34*, 3829.

[17] P. E. M. Siegbahn, *J. Am. Chem. Soc.* **1996**, *118*, 1487.

[18] Note that the apparent $\Delta E^{\neq}$ (activation energy)–ΔH (reaction enthalpy) correlation is just secondary and does not establish a cause and effect relationship between the two quantities. For details, see ref. [14c].

[19] As one can see in the discussion, the data also shows correlation of the relative barriers of the different substrates with ΔE_{st} of the bond being broken, e.g., in the series CH_4, SiH_4, GeH_4. For similar correlations, see a) S. Shaik, W. Wu, K. Dong, L. Song, P. C. Hiberty, *J. Phys. Chem. A* **2001**, *105*, 8226; b) M.-D Su, S.-Y. Chu, *J. Am. Chem. Soc.* **1999**, *121*, 1045.

[20] R. Becerra, S. E. Boganov, M. P. Egorov, V. Ya. Lee, O. M. Nefedov, R. Walsh, *Chem. Phys. Lett.* **1996**, *250*, 111.

[21] a) J. E. Baggott, M. A. Blitz, H. M. Frey, R. Walsh, *J. Am. Chem. Soc.* **1990**, *112*, 8337; Note that, for the $Me_2Si + SiH_4$ case, the experimental activation barrier was found to be 0.3 kcal mol^{-1}, while my calculated barrier height is 6.3 kcal mol^{-1}. The reason for such a difference is presumably that the basis sets (LANL2DZ and LANL2DZdp) used in this work are not good enough for the silicon compounds. Obtaining better data for such a silylene/silylane insertion reaction requires further sophisticated computational studies, which are, however, beyond the scope of the present work.

[22] R. Becerra, M. P. Egorov, I. V. Krylova, O. M. Nefedov, R. Walsh, *Chem. Phys. Lett.* **2002**, *351*, 47.

[23] Reversibility of initial complex formation was found in the $H_2Si + SiH_4$ case: a) R. Becerra, I. W. Carpenter, G. W. Gutsche, K. D. King, W. D. Lawrance, W. S. Staker, R. Walsh, *Chem. Phys. Lett.* **2001**, *333*, 83; b) U. N. Alexander, K. D. King, W. D. Lawrance, *Phys. Chem. Chem. Phys.* **2001**, *3*, 3085; c) U. N. Alexander, K. D. King, W. D. Lawrance, *J. Phys. Chem. A* **2002**, *106*, 973.

[24] For the $Me_2Si + SiH_4$ case, see J. E. Baggott, M. A. Blitz, H. M. Frey, P. D. Lightfoot, R. Walsh, *Int. J. Chem. Kinet.* **1992**, *24*, 127.

[25] a) T. H. Dunning, Jr., P. J. Hay in *Modern Theoretical Chemistry* (Ed. H. F. Schaefer, III), Plenum, New York, **1976**, pp. 1–28; b) P. J. Hay, W. R. Wadt, *J. Chem. Phys.* **1985**, *82*, 270; P. J. Hay, W. R. Wadt, *J. Chem. Phys.* **1985**, *82*, 284; P. J. Hay, W. R. Wadt, *J. Chem. Phys.* **1985**, *82*, 299.

[26] a) A. D. Becke, *Phys. Rev. A*, **1988**, *38*, 3098; b) A. D. Becke, *J. Chem. Phys.* **1993**, *98*, 5648; c) C. Lee, W. Yang, R. G. Parr, *Phys. Rev. B* 1988, *37*, 785.

[27] C. E. Check, T. O. Faust, J. M. Bailey, B. J. Wright, T. M. Gilbert, L. S. Sunderlin, *J. Phys. Chem. A* **2001**, *105*, 8111.

[28] R. Krishnan, J. S. Binkley, R. Seger, J. A. Pople, *J. Chem. Phys.* **1980**, *72*, 650.

[29] a) K. Fukui, *J. Phys. Chem.* **1970**, *74*, 4161; b) C. Gonzalez, H. B. Schlegel, *J. Phys. Chem.* **1989**, *93*, 2154.

[30] Gaussian 98 (Revision C.02), M. J. Frisch, G. W. Trucks, H. B. Schlegel, G. E. Scuseria, M. A. Robb, J. R. Cheeseman, V. G. Zakrzewski, Montgomery, J. A. Jr., R. E. Stratmann, J. C. Burant, S. Dapprich, J. M. Millam, A. D. Daniels, K. N. Kudin, M. C. Strain, O. Farkas, J. Tomasi, V. Barone, M. Cossi, R. Cammi, B. Mennucci, C. Pomelli, C. Adamo, S. Clifford, J. Ochterski, G. A. Petersson, P. Y. Ayala, Q. Cui, K. Morokuma, D. K. Malick, A. D. Rabuck, K. Raghavachari, J. B. Foresman, J. Cioslowski, J. V. Ortiz, A. G. Baboul, B. B. Stefanov, Liu, G. Liashenko, A. Piskorz, Komaromi, I. P.; R. Gomperts, R. L. Martin, D. J. Fox, T. Keith, Al-M. A. Laham, C. Y. Peng, A. Nanayakkara, C. Gonzalez, M. Challacombe, P. M. W. Gill, B. Johnson, W. Chen, M. W. Wong, J. L. Andres, C. Gonzalez, Head-M. Gordon, E. S. Replogle, J. A. Pople, Gaussian, Inc., Pittsburgh, PA, **1998**.

[31] The present computational results showed that these activation barriers and enthalpies calculated at the CCSD(T)/LANL2DZdp//B3LYP/LANL2DZ level are not significantly different from those computed at the B3LYP/LANL2DZ level. Using identical hardware and software, each CCSD/LANL2DZdp single-point calculation took an average of more than 73 times longer to complete than a B3LYP/LANL2DZ single-point calculation on the same geometry. Since the qualitative features of the potential energy profiles of the B3LYP and CCSD levels are similar to each other, the use of the former is sufficient to provide qualitatively correct results. Moreover, comparative studies are very useful in understanding similarities and differences in the chemical properties of compounds. In such cases, trends in the properties of interest can often be more important than their absolute values. While making such comparisons, the properties can be studied as a function of substituents, or periodic trends can be examined by studying the properties of compounds with elements from the same period or group. These options provide a criterion for testing the consistency of a given level of calculation. In addition, this method also allows properties to be predicted for compounds that are not yet amenable to experiment.

Received: April 27, 2004
Revised: August 17, 2004
Published online: October 28, 2004

